Available online at www.sciencedirect.com
ScienceDirect
Trans. Nonferrous Met. Soc. China 30(2020) 1091−1101
Transactions of Nonferrous Metals Society of China
www.tnmsc.cn

Electrochemical mechanism and flotation of chalcopyrite and galena in the presence of sodium silicate and sodium sulfite

Ye ZHANG[1,2], Run-qing LIU[1,2], Wei SUN[1,2], Li WANG[1,2], Yan-hong DONG[3], Chang-tao WANG[1,2]

1. School of Minerals Processing and Bioengineering, Central South University, Changsha 410083, China;
2. Key Laboratory of Hunan Province for Clean and Efficient Utilization of Strategic Calcium-containing Mineral Resources, Central South University, Changsha 410083, China;
3. Hunan Research Institute for Nonferrous Metals, Changsha 410100, China

Received 27 June 2019; accepted 18 February 2020

Abstract: The electrochemical mechanism involved in the selective separation of chalcopyrite from galena was investigated by flotation and electrochemical methods in the presence of sodium sulfite and sodium silicate, respectively, as a single depressant and their mixture as a combined depressant. Flotation tests revealed that the floatability of chalcopyrite was unaffected by depressants and its recovery remained constant (>80%) within the studied dosage range. Galena flotation was severely depressed with descending depressing order as follows: combined depressant > sodium silicate > sodium sulfite. Electrochemical analysis confirmed the high affinity of depressants on the galena surface, resulting in the formation of hydrophilic species, such as lead sulfite, lead sulfate, and lead orthosilicate. The oxidation of chalcopyrite surface and depressants did not exhibit any signals; conversely, the self-oxidation of chalcopyrite was depressed. The results of cyclic voltammograms well agreed with flotation results, demonstrating that chalcopyrite primarily reacted with the collector O-isopropyl-N-ethyl thionocarbamate and that galena mostly reacted with depressants.

Key words: flotation electrochemistry; chalcopyrite; galena; sodium sulfite; sodium silicate

1 Introduction

Chalcopyrite, as the major copper source from secondary mineral deposits, is the most abundant copper sulfide mineral accounting for nearly 70% of the total copper reserves globally [1−4]. Galena, the lead sulfide mineral, is the main source of lead metal worldwide with current production of more than 4.35×10^6 t [5,6]. Chalcopyrite and galena are usually associated in natural ore deposits. With the rapid decrease of high grade and large disseminated copper−lead ores owing to growing exploitation and usage, utilizing low-grade and complicatedly disseminated copper−lead ores is a promising option but poses a difficult task in mineral processing [7−10]. Sulfide minerals, such as chalcopyrite and galena, are well-known semiconductors and can accept or donate electrons [11,12]. Electrons are transferred when sulfide minerals are in contact with reagents, leading to the redox reaction of sulfide minerals. The products could affect the surface hydrophilic and hydrophobic properties of the sulfide minerals. Therefore, the electrochemical study of chalcopyrite and galena in different depression systems is useful

Foundation item: Project (51374247) supported by the National Natural Science Foundation of China; Project (2015CX005) supported by Innovation Driven Plan of Central South University, China; Project (B14034) supported by the National "111" Project, China; Project supported by the Open Sharing Fund for Large-scale Instruments and Equipment of Central South University and Collaborative Innovation Center for Clean and Efficient Utilization of Strategic Metal Mineral Resources, China

Corresponding author: Run-qing LIU; Tel: +86-13875851194; E-mail: liurunqing@126.com

DOI: 10.1016/S1003-6326(20)65280-3

in optimizing the separation of chalcopyrite from galena.

The hydrophobicity of sulfide minerals in electrochemically controlled conditions has been an area of concern in the last few decades [13,14]; the flotation and depression behavior of sulfide minerals has been studied using mixed potential mechanisms [15−17]. The maximum value of floatability of sulfide minerals at moderately oxidizing potentials is achieved given the formation of the hydrophobic sulfur [18−20]. However, the value decreases at reducing and highly oxidizing potentials owing to the unoxidized surface and the formation of hydrophilic metal hydroxide [21,22]. Oxidation constitutes a central part of the electrochemical reactivity of sulfide minerals in flotation systems based on the electrochemical theory [23]. Oxygen reduction affects the oxidation of sulfide minerals and the interactions with collectors, which has a pronounced effect on the flotation behavior of sulfide minerals [24,25]. Therefore, it is necessary to understand the mechanism of flotation separation between chalcopyrite and galena by using electrochemical methods.

In recent years, some electrochemical methods for chalcopyrite flotation and galena depression have been studied. Electrochemical methods provide useful information on the oxidizing/reducing characteristics of sulfide minerals. The electrochemical oxidation of chalcopyrite in the absence of any collector was studied by FAIRTHORNE et al [21] using zeta potential measurements and X-ray photoelectron spectroscopy. The hydrophobicity of chalcopyrite surface depends on two processes, namely, the iron and copper ion dissolution producing a sulfur-rich hydrophobic surface and metal hydroxide precipitation producing a hydrophilic surface. Therefore, the hydrophobicity of chalcopyrite may be controlled by the kinetics of formation and precipitation of these metal hydroxides. The redox behavior of galena in alkaline conditions has been investigated by GULER [26]. Pb-oxyhydroxides are released on the electrode along with sulfoxy species during the anodic process, whereas oxygen-containing Pb-species are reduced to metallic lead at highly reducing potentials. At a relative low potential, the surface of galena is oxidized to produce elemental sulfur, resulting in collectorless flotation. At a high potential, the surface of galena is oxidized to produce lead sulfide at pH=6, lead thiosulphate at pH=9, and lead hydroxide and sulfite at pH>12 [27].

Many studies have been conducted on inorganic depressants, such as sodium silicate and sodium sulfite, in the flotation of chalcopyrite and galena. In aqueous solutions, sodium silicates have three major species, including monomeric, polymeric, and colloidal species [28−30]. The role of each species in the depression mechanism was studied by some researchers [31,32]. These studies showed that the polymeric sodium silicate solution exhibits a high depression effect because it can cover a large surface of the mineral due to its weight and size. HOUOT and DUHAMET [33] reported that the good selectivity for copper sulfide can be achieved from other sulfides by using sodium sulfite in the flotation of sulfide ores with dialkyl-thionocarbamate as the collector. However, few studies have reported the electrochemical behavior of sodium silicate and sodium sulfite and their combined effects on depressing galena; this method may be a new non-toxic technique for separating chalcopyrite from galena.

In the present study, the electrochemical characteristics of chalcopyrite and galena in distinct systems of depressants and flotation tests were investigated. Electrochemical analyses were used to characterize the products of the oxidation and reduction of galena and chalcopyrite and the strong-to-weak sequence of interaction between combined depressants and chalcopyrite/galena. The results for the separation of chalcopyrite and galena were verified via flotation tests.

2 Experimental

2.1 Mineral samples

Chalcopyrite and galena were obtained from Tongling, Anhui Province and Fankou lead−zinc mine, Guangdong Province, respectively. Analytical work on the mineral samples showed the purity of chalcopyrite (94.62%) and galena (94.95%). The X-ray powder diffraction (XRD) patterns of chalcopyrite and galena are shown in Fig. 1. Mineral lumps were handpicked, crushed, ground in a ceramic ball mill, and sieved by screening. The mineral samples with particle size of 0.038−0.074 mm were used for micro-flotation tests.

These samples were stored in sealed glass bottles kept in a vacuum oven and ultrasonically washed in deionized water for several times before use.

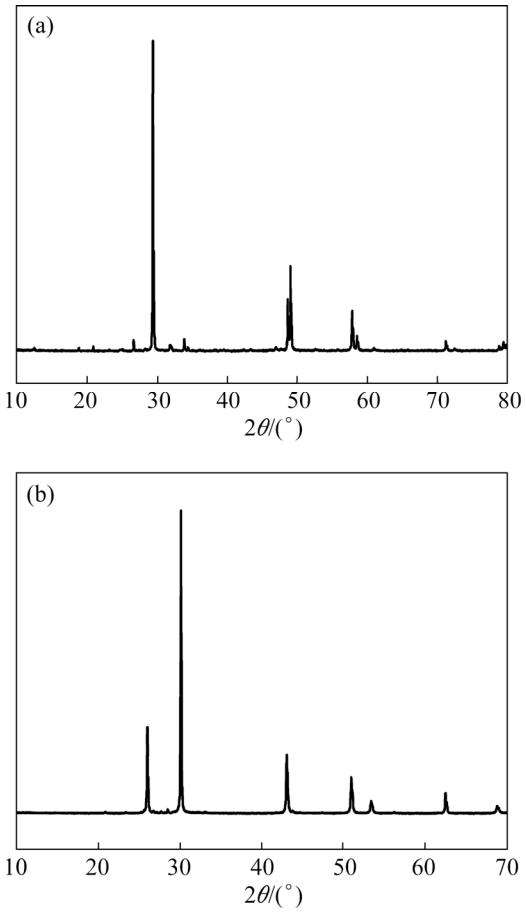

Fig. 1 X-ray diffraction patterns of chalcopyrite (a) and galena (b)

2.2 Flotation tests

Chalcopyrite and galena were subjected to single-mineral flotation tests in a 40 mL XFG type hitch groove flotation machine at a rotating speed of 1800 r/min. Flotation was conducted using 2.0 g of mineral sample and 35 mL of distilled water on a TCX-SOW type ultrasonic cleaner to remove the surface oxides. Thereafter, the sample was transferred to a flotation cell for further processing. pH was adjusted to 8.5−9 using HCl and NaOH. The systematic flotation flowsheet shown in Fig. 2 comprises the copper–lead bulk flotation, reagent removal, and copper–lead separation in practical application. In the first step, butyl xanthate was used to recover chalcopyrite and galena. In the second step, Na_2S was used to remove the residue butyl xanthate, with O-isopropyl-N-ethyl thionocarbamate (IPETC) as the collector. Flotation recovery (R) was calculated from $R=m_1/(m_1+m_2)\times 100\%$, where m_1 and m_2 are masses of the floated and un-floated fractions, respectively. All the tests were conducted in triplicates and thus the results presented in this work are average values with the standard deviation.

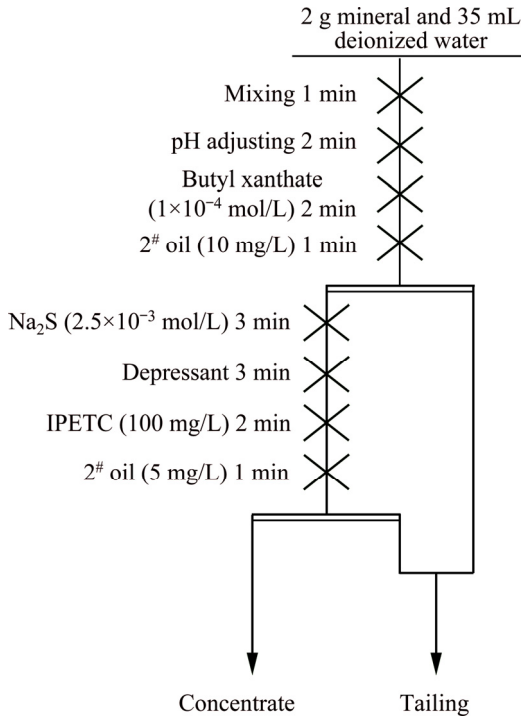

Fig. 2 Proposed flotation flowsheet

2.3 φ_h–pH diagrams

Potential (φ_h) vs pH diagrams are useful for understanding complex systems involving various chemical/electrochemical components. φ_h–pH diagrams of a distinct system at 25 °C in the present work were constructed with thermodynamic data from Ref. [34] and the HSC Chemistry software, version 5.0. φ_h is based on the standard hydrogen electrode and its unit is V.

2.4 Electrochemical measurements

Model 283 electrochemical system from Princeton EG&G PARC company in America was used for electrochemical measurements. Potentials were measured against the standard hydrogen electrode. Power CV models from Powersuit workstation was used for cyclic voltammetry analysis in a standard three-electrode cell. The electrochemical setup involved a standard three-electrode cell by using a selected sulfide mineral electrode as the working electrode, Ag/AgCl electrode as the reference electrode, and a graphite electrode as the auxiliary electrode. The

mineral electrodes were fabricated using pure chalcopyrite and galena crystals. The saturated Ag/AgCl electrode was used as the reference electrode with a potential value of 0.222 V against the normal hydrogen electrode at 25 °C. All solutions were mixed in deionized water. The potential of the working electrode was measured against the reference electrode coupled to a Luggin capillary filled with a saturated solution of KNO_3 (0.1 mol/L) as the supporting electrolyte. All measurements were made at ambient temperature. Reproducibility was ensured by controlling the electrode potential to stabilize for approximately 15 min before starting each measurement. In the experiments, the oxidation reduction potential of the slurry was measured directly after flotation.

Voltammetry was carried out in buffer solutions at pH 9.18. The cyclic voltammetry measurements were performed from the open circuit potential (OCP) to 900 mV (positive-going potential scan) and to −500 mV (negative-going potential scan) and back to OCP with a sweep rate of 20 mV/s.

3 Results and discussion

3.1 Flotation behavior

Figure 3 shows the flotation selectivity of chalcopyrite and galena with distinct depressant systems. As shown in Fig. 3(a), the flotation recovery of chalcopyrite was relatively higher than 80% in the whole range of sodium sulfite dosage. Thus, chalcopyrite was not depressed by sodium sulfite. The recovery of galena decreased progressively with the increasing dosage of sodium sulfite, reaching a minimum at approximately 30% when the dosage was more than 800 mg/L. The results indicated that sodium sulfite exhibits pronounced depressing selectivity toward galena. Therefore, it can be used as the depressant in the selective separation of chalcopyrite and galena.

Figure 3(b) shows that with the increasing dosage of sodium silicate, the recovery of chalcopyrite remained almost stable. However, the recovery of galena decreased continuously and reached 22.31% when the dosage of sodium silicate was higher than 1000 mg/L. The difference between the recovery of chalcopyrite and galena increased with increasing dosage. In contrast to the results in Fig. 3(a), the depressing effect of sodium silicate on galena was more intensive than that of sodium sulfite.

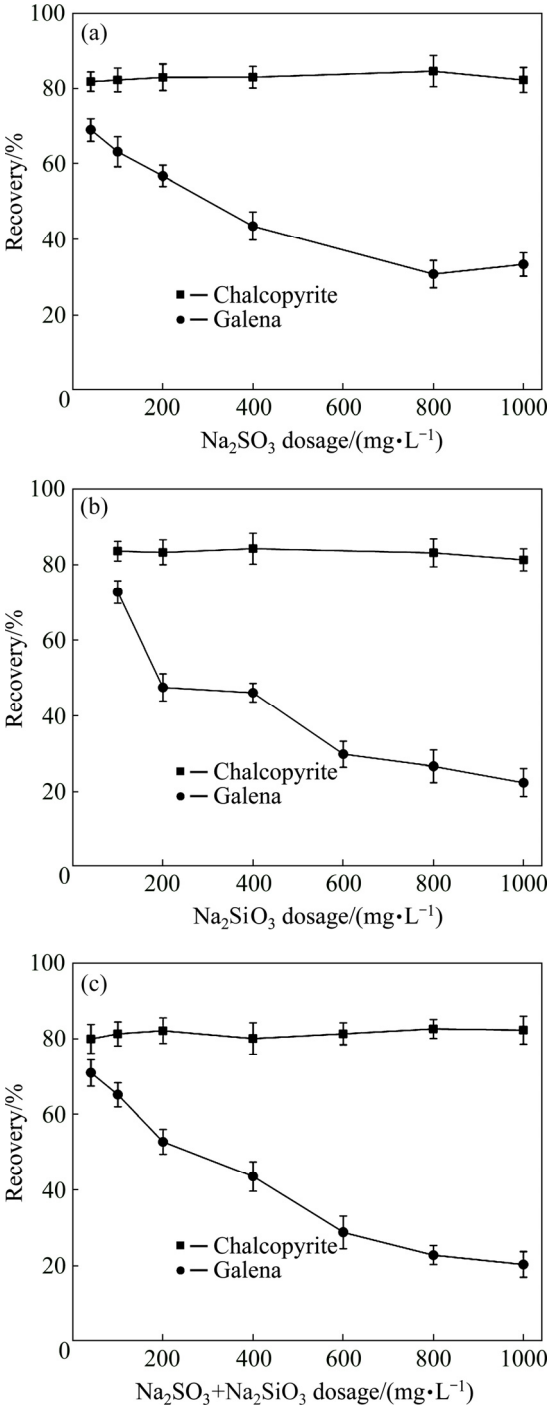

Fig. 3 Recovery of chalcopyrite and galena as function of different depressant systems: (a) Sodium sulfite; (b) Sodium silicate; (c) Combined depressant ([IPETC]= 100 mg/L, [2# oil] =5 mg/L, pH=8.5−9.0)

Figure 3(c) shows the effect of the dosage of combined depressant on the flotation recovery of chalcopyrite and galena. With the increased dosage of the combined depressant, chalcopyrite recovery

remained stable, whereas the recovery of galena decreased gradually during the whole range of dosage. At a dosage of 1000 mg/L, the separation effect between chalcopyrite and galena was enhanced, with 82.37% and 20.32% flotation recovery, respectively. The depressing effect of the combined system on galena was more intensive than that of single sodium sulfite and sodium silicate.

3.2 Electrochemical mechanism

3.2.1 Electrochemical studies in single system of sodium sulfite

Figure 4 shows the φ_h–pH diagrams for the systems of chalcopyrite–sodium sulfite–water, and galena–sodium sulfite–water. In the sodium sulfite system, hydrophobic products CuS occurred on the surface of chalcopyrite within a wide range of potential. The hydrophilic products $PbSO_3$ or $PbSO_4$ existed on the galena surface. Cu^{2+} or Fe^{2+} produced by the dissolution of chalcopyrite surface did not interact with SO_3^{2-}. Thus, it existed as ion in acidic conditions and as hydroxide in alkaline conditions. By contrast, Pb^{2+} was produced by the dissolution of galena surface interacting with SO_3^{2-}. $PbSO_3$ was produced, which may be further oxidized into $PbSO_4$. Hydration occurred under this circumstance, that is, the hydrophilic product $PbSO_4$ could probably interact with water molecules to form layers of adsorbed water molecules. This phenomenon is possible through hydrogen bonding with their surface oxygen. Hence, collector adsorption and adhesion between air bubbles were hindered, resulting in the depression of galena flotation.

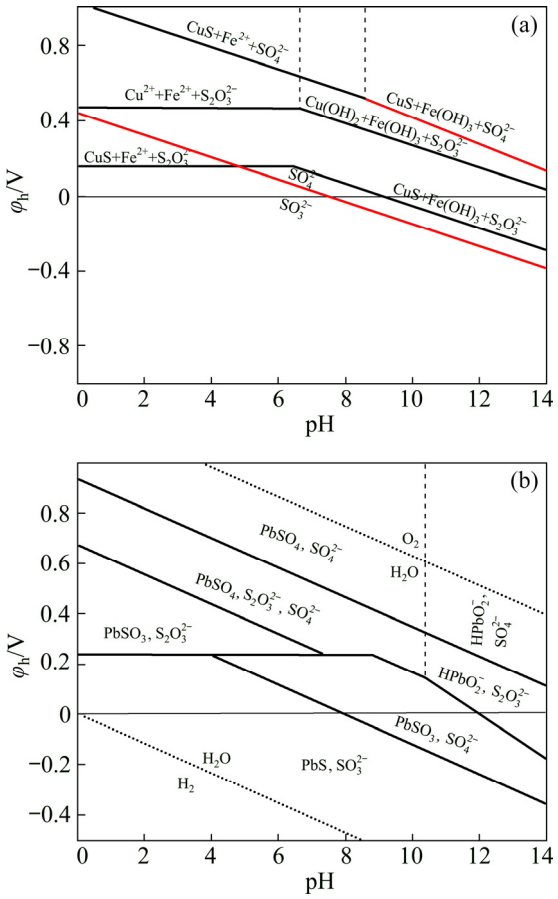

Fig. 4 φ_h–pH diagrams of chalcopyrite–sodium sulfite–water system (a) and galena–sodium sulfite–water system (b) at 25 °C (Equilibrium lines correspond to dissolved species at 10^{-4} mol/L and $[Na_2SO_3]$= 0.0159 mol/L)

Figure 5(a) shows the cyclic voltammetry results of the reaction of chalcopyrite with sodium sulfite and IPETC. In the blank solution (shown in line 1), two oxidation current peaks (1a, 1b) can be noted on the anodic scan and attributed to the self-oxidization of chalcopyrite. The first peak (1a) is attributed to $CuFeS_2$ oxidation (Eq. (1)). The

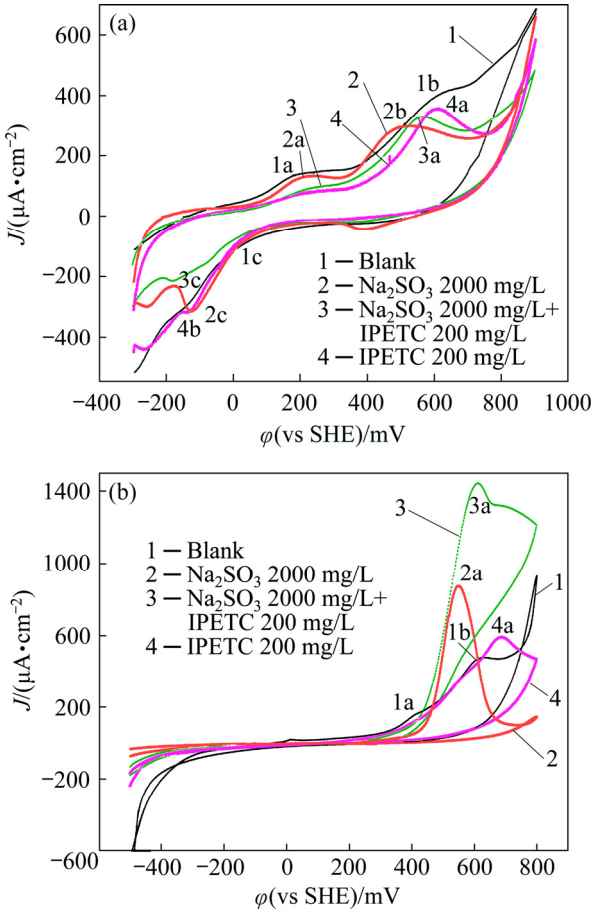

Fig. 5 Cyclic voltammograms of chalcopyrite (a) and galena (b) measured in pH 9.18 buffer solution with sodium sulfite and IPETC

second peak (1b) at approximately 600 mV may be attributed to CuS oxidation to S^0 (Eq. (2)). On the cathodic scan, a weak reduction peak (1c) was present at approximately 0 mV. The report [35] suggests that this peak resulted from the reverse reaction of Eq. (2).

$$CuFeS_2+3H_2O=CuS+Fe(OH)_3+S^0+3H^++3e \quad (1)$$

$$CuS+2H_2O=Cu(OH)_2+S^0+2H^++2e \quad (2)$$

In the solution of sodium sulfite, a new oxidation peak did not appear on the anodic scan. Meanwhile, the current value of the oxidation peak (2a, 2b) during the self-oxidization of chalcopyrite decreased. Thus, sodium sulfite depressed the oxidizing reaction of chalcopyrite. In addition, a reduction peak (2c) was observed at approximately 0 mV on the cathodic scan and may lead to chalcopyrite formation.

In the cyclic voltammogram of reaction of chalcopyrite with IPETC, the oxidation peak of Eq. (1) nearly disappeared, resulting from the adsorption of IPETC on the surface of chalcopyrite that depressed the oxidation reaction of chalcopyrite. One oxidation peak (4a) was observed at 600 mV on the anodic scan. The current value of the oxidation peak (4a) in the IPETC system was less than that of the second oxidation peak (1b) in the blank system. The shape of the oxidation peak in IPETC system was different from that of chalcopyrite. In addition to oxidation in Eq. (2), the reaction of chalcopyrite with IPETC might have also occurred. A previous report [36] indicated that at potentials higher than 0.31 V, chalcopyrite and IPETC will react, producing Cu−IPETC on the surface of chalcopyrite. This potential value is consistent with that of the oxidation peak in the diagram. A new weak reduction peak (4c) appeared between −50 and 150 mV on the cathodic scan, probably resulting from chalcopyrite production. In a mixed system of sodium sulfite and IPETC, the cyclic voltammogram was extremely similar to that of the IPETC system, demonstrating that IPETC played a leading role in the mixed system.

The cyclic voltammetry result of the reaction of galena with sodium sulfite and IPETC is shown in Fig. 5(b). In the blank system, two oxidation peaks (1a, 1b) were present and attributed to Eqs. (3) and (4). Given the absence of excess sulfur component, the reduction peak, which corresponds to galena production, did not appear on the cathodic scan. In the sodium sulfite system, only one oxidation peak (2a) was detected on the anodic scan probably representing Eq. (5). The reduction peak did not appear on the cathodic scan, showing the absence of a that there was no reaction of producing galena.

$$PbS+4H_2O=PbSO_4+8H^++8e \quad (3)$$

$$PbS+2H_2O=Pb(OH)_2+S^0+2H^++2e \quad (4)$$

$$PbS+SO_3^{2-}+5H_2O=PbSO_4+SO_4^{2-}+10H^++10e \quad (5)$$

In the IPETC solution, when the potential value was less than 600 mV, the cyclic voltammogram was similar to that in the blank system. Thus, galena self-oxidation occurred in the IPETC solution. The oxidation of galena was depressed slightly, which probably resulted from the low adsorption of IPETC on the surface of the mineral. However, when the scanning potential was more than 600 mV other than the phenomenon in the blank system, the current density of oxidation peak of galena (4a) continued to increase and peaked at 700 mV. Galena and lead ions do not react with IPETC [37]. Therefore, the shuffling of the oxidation peak value may be the result of the self-oxidation of the small amount of IPETC on the surface of galena.

In the mixed solution of sodium sulfite and IPETC, only one oxidation peak (3a) was observed at approximately 600 mV. When the potential value was less than 650 mV, the shape of oxidation peak was similar to that in the sodium sulfite system, demonstrating that in the reaction of mixed reagents, galena reacted with sodium sulfite in accordance with Eq. (5). However, when the potential was more than 650 mV as a result of IPETC addition, the shape of oxidation peak changed.

3.2.2 Electrochemical studies in single system of sodium silicate

Figure 6 shows the φ_h−pH diagrams for the Cu−Fe−Si−S−H_2O and Pb−Si−S−H_2O systems in single system of sodium silicate. Si existed in the form of $SiO(OH)_3^-$ in the Cu−Fe−Si−S−H_2O system and as $PbSiO_4$ and $SiO(OH)_3^-$ in the Pb−Si−S−H_2O system. Therefore, the selective depression of galena and chalcopyrite by sodium silicate may be attributed to the hydrophilic product $PbSiO_4$ produced on the galena surface. $PbSiO_4$ could adsorb on the mineral surface and interact with water molecules via hydrogen bonding with

surface oxygen. Consequently, layers of adsorbed water molecules were formed, thereby hindering collector adsorption and adhesion between air bubbles and the mineral particle. Therefore, the strong hydrophilic layers depressed the flotation of galena, but these reactions did not occur in the system of chalcopyrite. As such, sodium silicate cannot depress chalcopyrite flotation.

Figure 7(a) shows the comparison among the cyclic voltammograms of chalcopyrite in three different systems. In the blank system, the cyclic voltammogram of chalcopyrite has been explained. Two oxidation current peaks (4a, 4b) can be noted in the voltammogram of the system of sodium silicate on the anodic scan. The similar peak potential value to that of the blank system suggests the absence of oxidation interaction between sodium silicate and chalcopyrite. Compared with that in the blank system, the peak current density decreased, revealing that the addition of sodium silicate depressed chalcopyrite oxidation. The anodic scanning curve in the mixed system was extremely similar to that in the IPETC system, suggesting that IPETC was dominated in the mixed system.

Figure 7(b) shows the cyclic voltammetry results of galena in three distinct systems. The cyclic voltammogram in the blank system has been explained above. In the sodium silicate system, two oxidation current peaks (2a, 2b) were observed. The potential–pH diagram of the Pb−Si−S−H_2O system suggests that the first peak (2a) should be attributed to Eqs. (6) and (7). The second peak (2b) may be attributed to the oxidation reaction (Eq. (8)) leading to lead silicate and sulfate formation.

$$2PbS+SiO(OH)_3^-=Pb_2SiO_4+2S^0+3H^++4e \quad (6)$$

$$Pb_2SiO_4+SiO(OH)_3^-=2PbSiO_4+Pb(OH)_2+3H^++4e \quad (7)$$

$$2PbS+SiO(OH)_3^-+8H_2O= Pb_2SiO_4+2SO_4^{2-}+19H^++16e \quad (8)$$

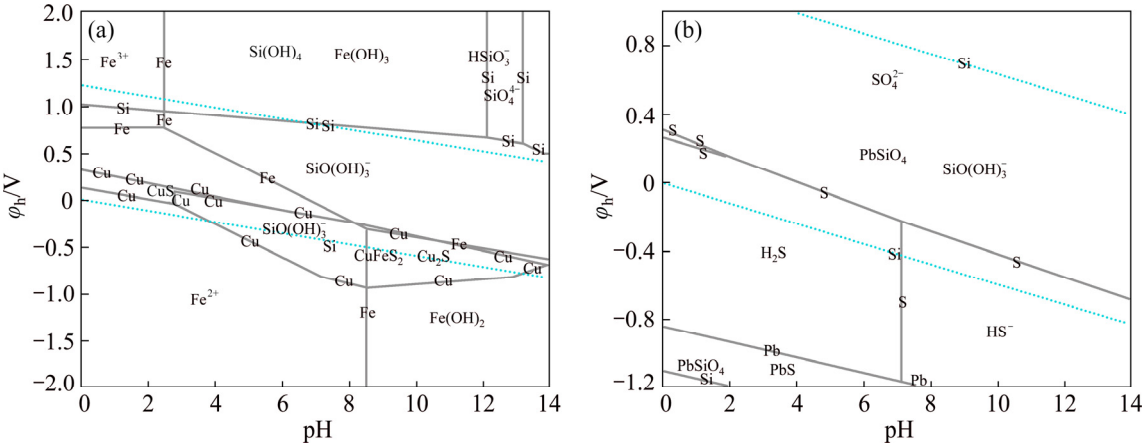

Fig. 6 φ_h–pH diagram of Cu−Fe−Si−S−H_2O system (a) and Pb−Si−S−H_2O system (b) at 25 °C in single system of sodium silicate ([Si]=0.0149 mol/L, [S]=10^{-4} mol/L, [Fe]=10^{-4} mol/L, [Cu]=10^{-4} mol/L, [Pb]=10^{-4} mol/L)

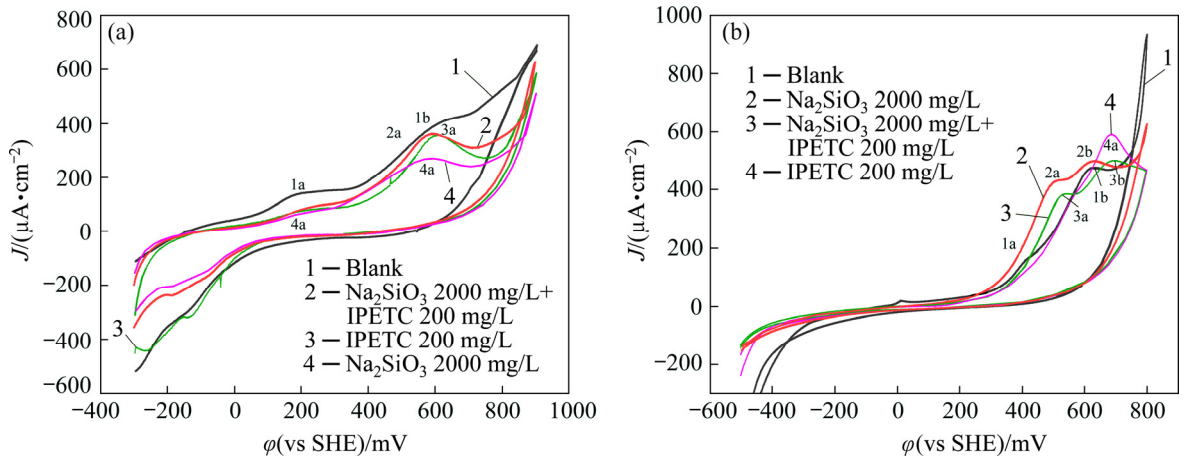

Fig. 7 Cyclic voltammograms of chalcopyrite (a) and galena (b) measured in pH 9.18 buffer solution with sodium silicate and IPETC

Compared with the voltammogram in the sodium silicate system, the current density of the first anodic peak (3a) decreased in the mixed system of IPETC and sodium silicate. Thus, IPETC depressed the interaction between galena and sodium silicate. The peak values of the two anodic peaks (3a, 3b) in the mixed system were identical with those in the sodium silicate system, revealing that the reactions (Eqs. (6)−(8)) still occurred in the mixed solution of IPETC and sodium silicate.

3.2.3 Electrochemical studies in combined system of sodium sulfite and sodium silicate

Figure 8 shows the φ_h−pH diagrams for the Cu−Fe−Si−S−H_2O and Pb−Si−S−H_2O systems in combined system of sodium sulfite and sodium silicate. The combined system involving 0.0159 mol/L SO_3^{2-} and 0.0149 mol/L SiO_3^{2-}, Pb primarily existed in the form of $PbSiO_4$ in the Pb−Si−S−H_2O system, while Fe/Cu orthosilicate or silicate did not form in the Cu−Fe−Si−S−H_2O system.

Figure 9(a) shows the cyclic voltammograms of the interaction between chalcopyrite and the combined depressant system. Under the effects of these two kinds of reagents, new anodic peaks did not appear on the anodic scan, showing that no new oxidation occurred under the mutual effect of sodium sulfite and sodium silicate. The first anodic peak (3a) in the solution of sodium sulfite and sodium silicate nearly coincides with that in the solution of sodium sulfite (4a). Thus, when the potential value is less than 250 mV, sodium sulfite is dominated in the mixed reagent. The shape of the second oxidation peak (3b) in the solution of sodium sulfite and sodium silicate is similar to that in sodium sulfite (4b). Meanwhile, the current density of peak in the solution of sodium sulfite and sodium silicate was larger than that in sodium sulfite. These phenomena indicate that sodium silicate and sodium sulfite had reacted with

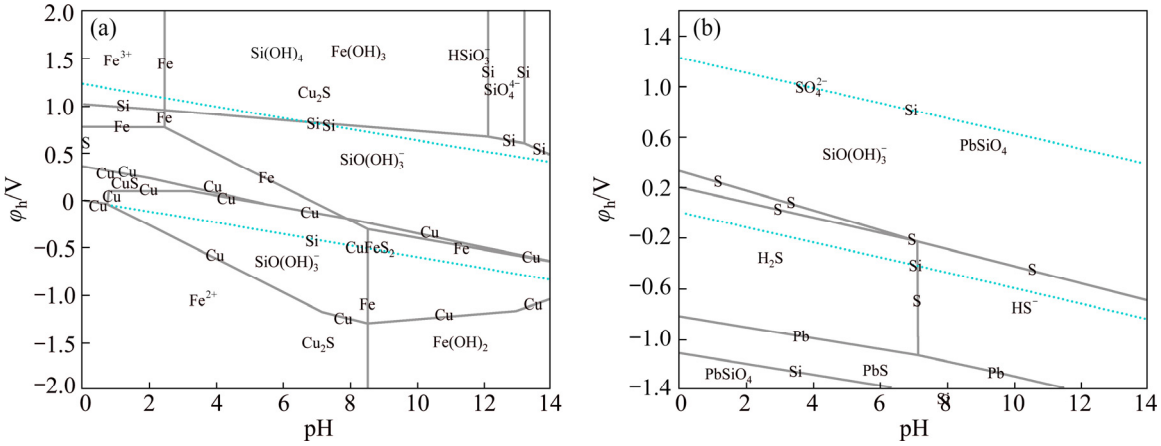

Fig. 8 φ_h−pH diagram of Cu−Fe−Si−S−H_2O system (a) and Pb−Si−S−H_2O system (b) at 25 °C in combined system of sodium sulfite and sodium silicate ([Si]=0.0149 mol/L, [S]=0.0159 mol/L, [Fe]=10^{-4} mol/L, [Cu]=10^{-4} mol/L, [Pb]=10^{-4} mol/L)

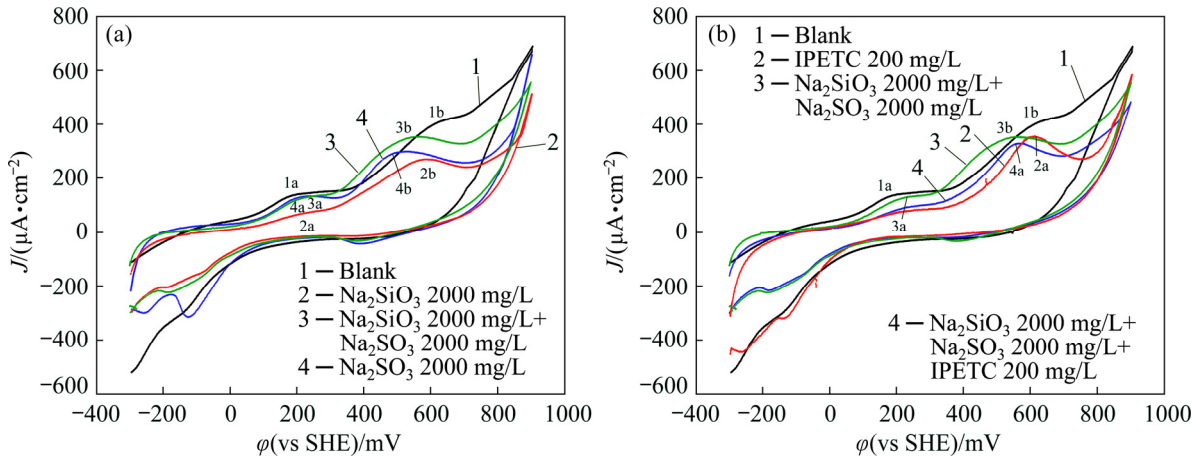

Fig. 9 Cyclic voltammograms of chalcopyrite measured in pH 9.18 buffer solution with Na_2SO_3+Na_2SiO_3 and IPETC

chalcopyrite. Figure 9(b) shows the cyclic voltammograms of chalcopyrite in a mixed solution of combined depressants and IPETC. These curves show that the scanning curve of the reaction of chalcopyrite with combined depressants and IPETC was similar that of the interaction between chalcopyrite and IPETC.

Figure 10(a) shows the cyclic voltammograms of galena in the sodium sulfite and sodium silicate solutions. The cyclic voltammogram of the reaction of galena with sodium sulfite and sodium silicate nearly coincided with that of the interaction between galena and sodium silicate. As such, sodium silicate was dominated in this system. Curve 2 was compared with curve 4, and the peak potential value of the interaction between sodium silicate and galena was less than that of the interaction between sodium sulfite and galena. This phenomenon is attributed to the lead orthosilicate produced by the interaction between sodium silicate and galena that adsorbed on the surface of the mineral and inhibited the interaction between sodium sulfite and galena. The φ_h−pH diagram for the Pb−Si−S−H_2O system (Fig. 8(b)) shows that lead primarily exists in the form of lead orthosilicate in this system. As such, the oxidation reaction of galena and sodium silicate occurred in this system.

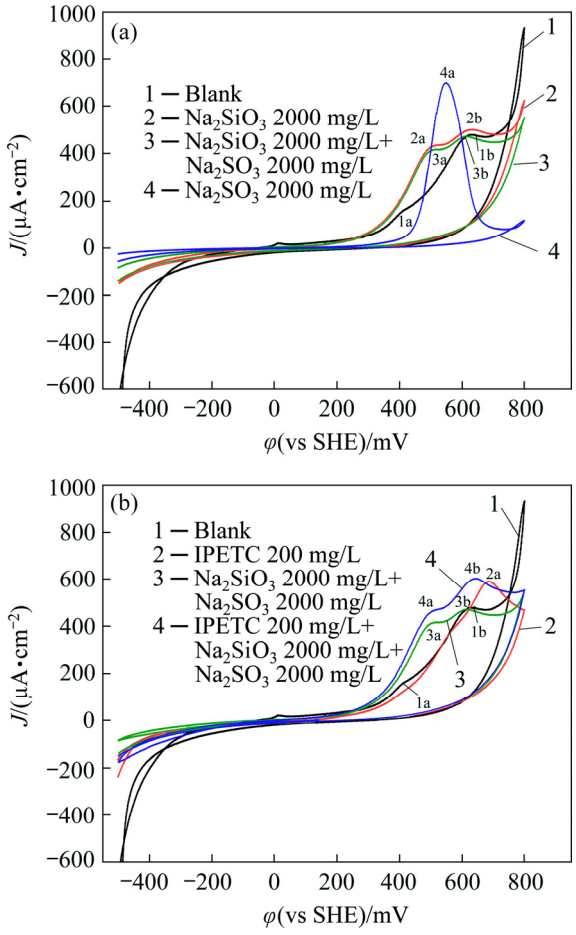

Fig. 10 Cyclic voltammograms of galena measured in pH 9.18 buffer solution with Na_2SO_3+Na_2SiO_3 and IPETC

IPETC was added in this mixed system, and the cyclic voltammograms of galena are shown in Fig. 10(b). As shown in the figure (curve 4), two oxidation peaks (4a, 4b) appeared on the anodic scan and the peak value was the same as that in the system of sodium sulfite and sodium silicate (3a, 3b). IPETC increased the current density of the peak. The shape and the potential value of the peak were similar to those in the system of sodium sulfite and sodium silicate, indicating that sodium sulfite and sodium silicate were dominated in this system.

4 Conclusions

(1) The flotation results showed that the floatability of chalcopyrite was hardly depressed by all three kinds of depressants and its recovery remained stable (more than 80%) in the whole range of depressant dosage. However, all these depressants showed a negative effect on the flotation of galena with the following descending depressing order: combined depressant > sodium silicate > sodium sulfite.

(2) Cyclic voltammetry measurements showed that in the presence of reagents, hydrophilic species (e.g., lead sulfite, lead sulfate, and lead orthosilicate) formed on the galena surface under low and high potential conditions were responsible for its depression. No evidence suggests the presence of chemical species on the chalcopyrite surface after its interaction with depressants, resulting in the improved floatation of chalcopyrite. Therefore, the results of cyclic voltammograms are consistent with the flotation results, demonstrating that chalcopyrite primarily reacted with IPETC and galena mostly reacted with a depressant.

References

[1] GUAN Qing-jun, SUN Wei, HU Yue-hua, YIN Zhi-gang, ZHANG Chen-hu, GUAN Chang-ping, ZHU Xiang-nan, KHOSO S A. Simultaneous control of particle size and morphology of α-$CaSO_4\cdot\frac{1}{2}H_2O$ with organic additives [J]. Journal of the American Ceramic Society, 2019, 102:

2440−2450.

[2] KHOSO S A, HU Yue-hua, LÜ Fei, GAO Ya, LIU Run-qing, SUN Wei. Xanthate interaction and flotation separation of H_2O_2-treated chalcopyrite and pyrite [J]. Transactions of Nonferrous Metals Society of China, 2019, 29(12): 2604−2614.

[3] MA Xin, WANG Shuai, ZHONG Hong. Sodium benzyl trithiocarbonate synthesis and flotation performance to chalcopyrite [J]. The Chinese Journal of Nonferrous Metals, 2018, 28(5): 1067−1075. (in Chinese)

[4] CHANG Ke-xin, ZHANG Yan-sheng, ZHANG Jia-ming, LI Teng-fei, WANG Jun, QIN Wen-qing. Effect of temperature-induced phase transitions on bioleaching of chalcopyrite [J]. Transactions of Nonferrous Metals Society of China, 2019, 29(10): 2183−2191.

[5] FLORES-ALVAREZ J M, ELIZONDO-ALVAREZ M A, DAVILA-PULIDO G I, GUERRERO-FLORES A D, URIBE-SALAS A. Electrochemical behavior of galena in the presence of calcium and sulfate ions [J]. Minerals Engineering, 2017, 111: 158−166.

[6] LAN Li-hong, CHEN Jian-hua, LI Yu-qiong, LAN Ping, YANG Zhuo, AI Guang-yong. Microthermokinetic study of xanthate adsorption on impurity-doped galena [J]. Transactions of Nonferrous Metals Society of China, 2016, 26(1): 272−281.

[7] BU Yong-jie, HU Yue-hua, SUN Wei, GAO Zhi-yong, LIU Run-qing. Fundamental flotation behaviors of chalcopyrite and galena using O-isopropyl-N-ethyl thionocarbamate as a collector [J]. Minerals, 2018, 8: 115.

[8] ZHANG Ye, HU Yue-hua, SUN Ning, LIU Run-qing, WANG Zhen, WANG Li, SUN Wei. Systematic review of feldspar beneficiation and its comprehensive application [J]. Minerals Engineering, 2018, 128: 141−152.

[9] MA Yi-wen, HAN Yue-xin, ZHU Yi-min, LI Yan-jun, LIU Hao. Flotation behaviors and mechanisms of chalcopyrite and galena after cyanide treatment [J]. Transactions of Nonferrous Metals Society of China, 2016, 26(12): 3245−3252.

[10] BAMPOLE D L, LUIS P, MULABABAFUBIANDI A F. Sustainable copper extraction from mixed chalcopyrite–chalcocite using biomass [J]. Transactions of Nonferrous Metals Society of China, 2019, 29(10): 2170−2182.

[11] ZHANG Ye, HU Yue-hua, WANG Li, SUN Wei. Systematic review of lithium extraction from salt-lake brines via precipitation approaches [J]. Minerals Engineering, 2019, 139: 1−14.

[12] LI Yu-qiong, CHEN Jian-hua, LAN Li-hong, GUO Jin. Adsorption of O_2 on pyrite and galena surfaces [J]. The Chinese Journal of Nonferrous Metals, 2012, 22(4): 1184−1194. (in Chinese)

[13] GULER T, HICYILMAZ C. Hydrophobicity of chalcopyrite with dithiophosphate and dithiophosphinate in electrochemically controlled condition [J]. Colloids and Surfaces A: Physicochemical and Engineering Aspects, 2004, 235: 11−15.

[14] GULER T, HICYILMAZ C, GOKAGAC G, EKMEKCI Z. Voltammetric and drift spectroscopy investigation in dithiophosphinate−chalcopyrite system [J]. J Colloid Interface Sci, 2004, 279: 46−54.

[15] HU Yue-hua, SUN Wei, WANG Dian-zuo. Electrochemistry of flotation of sulphide minerals [M]. Beijing: Tsinghua University Press, 2009.

[16] TADIE M, CORIN K C, WIESE J G, NICOL M, O'CONNOR C T. An investigation into the electrochemical interactions between platinum group minerals and sodium ethyl xanthate and sodium diethyl dithiophosphate collectors: Mixed potential study [J]. Minerals Engineering, 2015, 83: 44−52.

[17] LI Shuang-ke, GU Guo-hua, QIU Guan-zhou, CHEN Zhi-xiang. Flotation and electrochemical behaviors of chalcopyrite and pyrite in the presence of N-propyl-N′-ethoxycarbonyl thiourea [J]. Transactions of Nonferrous Metals Society of China, 2018, 28(6): 1241−1247.

[18] GRANO S R, SOLLAART M, SKINNER W, PRESTIDGE C A, RALSTON J. Surface modifications in the chalcopyrite-sulphite ion system. I: Collectorless flotation, XPS and dissolution study [J]. International Journal of Mineral Processing, 1997, 50: 1−26.

[19] GRANO S R, CNOSSEN H, SKINNER W, PRESTIDGE C A, RALSTON J. Surface modifications in the chalcopyrite-sulphite ion system. II: Dithiophosphate collector adsorption study [J]. International Journal of Mineral Processing, 1997, 50: 27−45.

[20] SUN Wei, SUN Chen, LIU Run-qing, CAO Xue-feng, TAO Hong-biao. Electrochemical behavior of galena and jamesonite flotation in high alkaline pulp [J]. Transactions of Nonferrous Metals Society of China, 2016, 26(2): 551−556.

[21] FAIRTHORNE G, FORNASIERO D, RALSTON J. Effect of oxidation on the collectorless flotation of chalcopyrite [J]. International Journal of Mineral Processing, 1997, 49: 31−48.

[22] ZHANG Ye, WANG Li, SUN Wei, HU Yue-hua, TANG Hong-hu. Membrane technologies for Li^+/Mg^{2+} separation from salt-lake brines and seawater: A comprehensive review [J]. Journal of Industrial and Engineering Chemistry, 2020, 81: 7−23.

[23] FUERSTENAU M C, KUHN M C, ELGILLANI D A. The role of dixanthogen in xanthate flotation of pyrite [J]. Transactions of the American Institute of Mining, Metallurgical and Petroleum Engineers, 1968, 241: 148−156.

[24] BUCKLEY A N, WOODS R. The surface oxidation of pyrite [J]. Applied Surface Science, 1987, 27: 437−452.

[25] WANG Li, ZHANG Ye, SUN Ning, SUN Wei, HU Yue-hua, TANG Hong-hu. Precipitation methods using calcium-containing ores for fluoride removal in wastewater [J]. Minerals, 2019, 9(9): 511.

[26] GULER T. Redox behavior of galena in alkaline condition [J]. Ionics, 2018, 24: 221−227.

[27] KELSALL G H, YIN Q, VAUGHAN D J, ENGLAND K E R, BRANDON N P. Electrochemical oxidation of pyrite (FeS_2) in aqueous electrolytes [J]. Journal of Electroanalytical Chemistry, 1999, 471: 116−125.

[28] TOHRY A, DEHGHANI A. Effect of sodium silicate on the reverse anionic flotation of a siliceous–phosphorus iron ore [J]. Separation and Purification Technology, 2016, 164: 28−33.

[29] WANG Li, HU Guang-yan, SUN Wei, KHOSO S A, LIU

Run-qing, ZHANG Xiang-feng. Selective flotation of smithsonite from dolomite by using novel mixed collector system [J]. Transactions of Nonferrous Metals Society of China, 2019, 29(5): 1082−1089.

[30] ZHANG Ye, HU Yue-hua, SUN Ning, KHOSO S A, WANG Li, SUN Wei. A novel precipitant for separating lithium from magnesium in high Mg/Li ratio brine [J]. Hydrometallurgy, 2019, 187: 125−133.

[31] TIAN M, GAO Z, SUN W, HAN H, SUN L, HU Y. Activation role of lead ions in benzohydroxamic acid flotation of oxide minerals: New perspective and new practice [J]. J Colloid Interface Sci, 2018, 529: 150−160.

[32] SUN Wei, TANG Hong-hu, CHEN Chen. Solution chemistry behavior of sodium silicate in flotation of fluorite and scheelite [J]. The Chinese Journal of Nonferrous Metals, 2013, 23(8): 2274−2283. (in Chinese)

[33] HOUOT R, DUHAMET D. Floatability of chalcopyrite in the presence of dialkyl-thionocarbamate and sodium sulfite [J]. International Journal of Mineral Processing, 1993, 37: 273−282.

[34] WANG Dian-zuo, HU Yue-hua. Solution chemistry of flotation [M]. Changsha, China: Hunan Science and Technology Press, 1988. (in Chinese)

[35] PANG J, CHANDER S. Oxidation and wetting behavior of chalcopyrite in the absence and presence of xanthates [J]. Mining, Metallurgy & Exploration, 1990, 7: 149−155.

[36] WOODS R, HOPE G A. A SERS spectroelectrochemical investigation of the interaction of O-isopropyl-N-ethylthionocarbamate with copper surfaces [J]. Colloids and Surfaces A−Physicochemical and Engineering Aspects, 1999, 146: 63−74.

[37] FAIRTHORNE G, FORNASIERO D, RALSTON J. Interaction of thionocarbamate and thiourea collectors with sulphide minerals: A flotation and adsorption study [J]. International Journal of Mineral Processing, 1997, 50: 227−242.

黄铜矿与方铅矿在硅酸钠和亚硫酸钠体系中的浮选分离和电化学机理

张 烨[1,2]，刘润清[1,2]，孙 伟[1,2]，王 丽[1,2]，董艳红[3]，王长涛[1,2]

1. 中南大学 资源加工与生物工程学院，长沙 410083；
2. 中南大学 战略含钙矿物资源清洁高效利用湖南省重点实验室，长沙 410083；
3. 湖南有色金属研究院，长沙 410100

摘 要：通过浮选和电化学方法研究黄铜矿和方铅矿在硅酸钠、亚硫酸钠分别作为单一抑制剂以及混合抑制剂条件下选择性分离的电化学机理。浮选实验表明，黄铜矿可浮性不受抑制剂的影响，而且在实验的抑制剂用量范围内，黄铜矿的回收率基本不变(>80%)。方铅矿的浮选受到严重的抑制，抑制剂的抑制作用由强到弱的顺序为：混合抑制剂 > 单一硅酸钠 > 单一亚硫酸钠。电化学分析证明抑制剂在方铅矿表面作用强烈，产生亲水性物质，如亚硫酸铅、硫酸铅和正硅酸铅。电化学分析没有发现黄铜矿表面以及抑制剂的氧化，但发现黄铜矿的自我氧化作用被抑制。循环伏安结果与浮选结果非常吻合，表明黄铜矿主要与捕收剂 O-异丙基-N-乙基硫代氨基甲酸酯作用，而方铅矿主要与抑制剂作用。

关键词：浮选电化学；黄铜矿；方铅矿；亚硫酸钠；硅酸钠

(Edited by Xiang-qun LI)